Mar Geophys Res (2007) 28:101–107
DOI 10.1007/s11001-007-9017-6

ORIGINAL RESEARCH PAPER

Seismic velocities and quantification of gas-hydrates from AVA modeling in the western continental margin of India

Maheswar Ojha · Kalachand Sain

Received: 12 January 2006 / Accepted: 20 February 2007 / Published online: 31 March 2007

Abstract The most commonly used marker for the investigation of gas-hydrates is the bottom simulating reflector (BSR), which is caused by gas-hydrate laden sediment underlain by either brine or gas-saturated sediment. A BSR has been identified by seismic experiment in the Kerala-Konkan Basin of the western continental margin of India. Here we perform AVA modeling of seismic reflection data from a BSR to investigate the seismic velocities for quantitative assessment of gas-hydrates and to understand the origin of the BSR. The result reveals a *P*-wave velocity of 2.245 km/s and an *S*-wave velocity of 0.895 km/s for the sediments above the BSR. This corresponds to a Poisson ratio of 0.406 and hydrates saturation of ~30% in the study area. The comparison of estimated *P*-wave velocity (1.77 km/s) above the hydrates-bearing sediment to that (1.78 km/s) below the BSR implies that the origin of the BSR is mainly due to gas-hydrates, as the presence (even in small quantities) of free-gas reduces the *P*-wave velocity considerably.

Keywords Gas-hydrates · BSR · Seismic velocities · AVA modeling · Quantification

Introduction

Gas-hydrates are crystalline substances comprising water and methane, formed at high pressure and cool temperature, and found in permafrost and outer continental margins around the world (Sloan 1998; Henriet and Mienert 1998; Paul and Dillon 2001; Max 2003). Gas-hydrates have attracted the scientific community because of their potential as future energy resources, possible role in climate change, influence on submarine geo-hazard, and relationship to fluid flow in accretionary wedges. Therefore, quantification of gas-hydrates is very important for evaluating resource potential and assessing environmental hazards.

Gas-hydrates are mostly identified by mapping an anomalous reflector on seismic section, known as the bottom simulating reflector or BSR, which is often associated with the base of the gas-hydrates stability field in thermobaric chemical equilibrium. The BSR is caused either by the presence of gas-hydrate laden sediments underlain by free-gas bearing sediments, or by highly saturated gas-hydrates underlain by brine saturated sediments. Pure hydrates have much higher *P*- and *S*-wave seismic velocities than the host sediments or pore fluids. Hence the presence of gas-hydrates increases the seismic velocities that again depend upon the concentration of hydrates in the pore spaces of sediments. In contrast, even a small amount of free-gas below the gas-hydrates-bearing sediments causes a considerable drop in *P*-wave velocity, whereas the *S*-wave velocity remains almost unchanged compared to that of the background (in absence of gas-hydrates and free-gas) velocity. Therefore, accurate estimation of seismic velocities is required for translating the velocity build-up and/or drop across the BSR in terms of concentration of gas-hydrates and/or free-gas.

Due to the large contrast in elastic properties across the BSR, the reflection from the BSR is very strong and can be easily mapped on seismic data based on its characteristic features. For marine seismic data, the reflection from the BSR shows a large amplitude and opposite polarity with respect to the seafloor reflection. The BSR mimics the shape of seafloor and cuts across dipping strata. The

M. Ojha · K. Sain (✉)
National Geophysical Research Institute, Uppal Road, Hyderabad 500007, India
e-mail: kalachandsain@yahoo.com

amplitude versus angle (AVA) information can be used to determine *P*-wave velocity (V_P), *S*-wave velocity (V_S) and density (ρ) of both gas-hydrates and free-gas saturated sediments. Thus, estimation of both V_P and V_S or Poisson's ratio by AVA modeling provides vital input in assessing the amount of gas-hydrates and/or free-gas across a BSR. As the density across a BSR remains almost constant, the AVA variation is caused mainly by the *P*- and *S*-wave velocity change across the BSR.

In this study we perform AVA modeling using the multi-channel marine seismic reflection data from a BSR that has been identified in the Kerala-Konkan Basin of the western continental margin of India with a view to deriving both the V_P and V_S, and hence quantifying the amount of gas-hydrates and free-gas, if present.

Theory

Investigation of angle or offset-dependent reflectivity guided by Zoeppritz equations (Zoeppritz 1919) started a long time ago (e.g., Ostrander 1984; Castagna et al. 1993). This method is based on the determination of reflection and transmission coefficients or amplitudes for both *P*- and converted *S*-waves as a function of angle. When a seismic ray strikes a plane boundary obliquely, partition of energy takes place. Figure 1 illustrates the reflection, transmission and mode conversion of a plane *P*-wave at a boundary separated by three elastic parameters (V_P, V_S and ρ) on either side. For easy numerical solution, the Zoeppritz equations can be written through a matrix form (Waters 1977) as

$$\mathbf{Q} = \mathbf{P}^{-1}\mathbf{R} \tag{1}$$

where **P** is a 4 × 4 square matrix and, **R** and **Q** are 4 × 1 column matrices shown below.

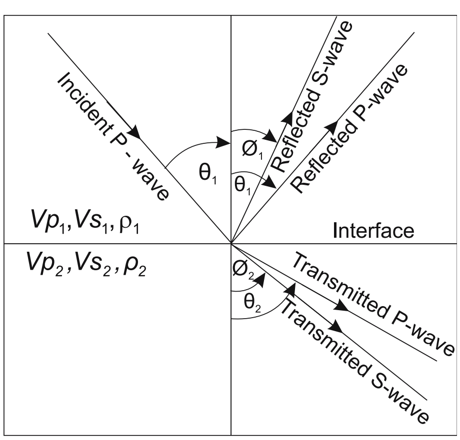

Fig. 1 Ray diagram for the partition of plane wave energy at a horizontal interface

$$\mathbf{P} = \begin{bmatrix} \sin\theta_1 & \cos\phi_1 & -\sin\theta_2 & \cos\phi_2 \\ -\cos\theta_1 & \sin\phi_1 & -\cos\theta_2 & \cos\phi_2 \\ \sin 2\theta_1 & \frac{V_{P1}}{V_{S1}}\cos 2\phi_1 & \frac{\rho_2}{\rho_1}\frac{V_{S2}^2}{V_{S1}^2}\frac{V_{P1}}{V_{P2}}\sin 2\theta_2 & -\frac{\rho_2}{\rho_1}\frac{V_{P1}}{V_{S1}}\frac{V_{S2}}{V_{P2}}\cos 2\phi_2 \\ \cos 2\phi_1 & -\frac{V_{S1}}{V_{P1}}\sin 2\phi_1 & -\frac{\rho_2}{\rho_1}\frac{V_{P2}}{V_{P1}}\cos 2\phi_2 & -\frac{\rho_2}{\rho_1}\frac{V_{S2}}{V_{P1}}\sin 2\phi_2 \end{bmatrix}$$

$$\mathbf{Q} = [\mathbf{R_{PPR}} \quad \mathbf{R_{PSVR}} \quad \mathbf{R_{PPT}} \quad \mathbf{R_{PSVT}}]^{\mathrm{T}} \text{ and}$$
$$\mathbf{R} = [\sin\theta_1 \quad \cos\theta_1 \quad \sin 2\theta_1 \quad \cos 2\phi_1]^{\mathrm{T}}$$

where $\mathbf{R_{PPR}}$ and $\mathbf{R_{PSVR}}$ are the reflection coefficients and, $\mathbf{R_{PPT}}$ and $\mathbf{R_{PSVT}}$ are transmission coefficients of P–P and converted P–S waves respectively. Angles (θ and ϕ) are defined in Fig. 1.

Using Eq. 1, we can calculate the amplitudes or reflection coefficients of reflected P–P and mode-converted P–S waves as a function of incident angle from BSR separated by three elastic parameters (V_P, V_S, and ρ) on either side.

Seismic velocity of gas-hydrates bearing sediments

A number of empirical relations exist to explain the variation of seismic velocities for gas-hydrates-bearing sediments. The three-phase weighted equation of Lee et al. (1996) for non-contact model in which hydrates are situated away from the grain contact and the effective medium theory of Helgerud et al. (1999) which is a contact model where hydrates are considered as part of the rock frame, are mostly used. We compute the seismic velocities of hydrates-bearing sediments using the three phase weighted equation of Lee et al. (1996), which is more convenient and more accurately predicts seismic velocities of gas-hydrates-bearing sediments (Lee and Collect 2001). The V_P of gas-hydrates saturated sediment is calculated as

$$\frac{1}{V_P} = \frac{W\phi(1-S)^n}{V_{P1}} + \frac{1 - W\phi(1-S)^n}{V_{P2}} \tag{2a}$$

where

$$\frac{1}{V_{P1}} = \rho_b\left(\frac{\phi(1-S)}{\rho_w V_w^2} + \frac{\phi S}{\rho_h V_h^2} + \frac{(1-\phi)}{\rho_m V_m^2}\right)$$

and

$$\frac{1}{V_{P2}} = \left(\frac{\phi(1-S)}{V_w} + \frac{\phi S}{V_h} + \frac{(1-\phi)}{V_m}\right)$$

where V_{P1} and V_{P2} are the *P*-wave velocities of hydrates-bearing sediments for three-phase Wood equation (Wood 1941) and three-phase time-average equation (Wyllie et al. 1958) respectively. W, ρ_b, ρ_w, ρ_h, ρ_m,ϕ, S, V_w, V_h, V_m and n are weighting factor, bulk density, density of water, density of gas-hydrates, density of matrix, porosity, gas-hydrates saturation, *P*-wave velocity in water, *P*-wave velocity of pure gas-hydrates, P-wave velocity of matrix and a lithification constant respectively. The bulk density of sediments can be calculated as

$$\rho_b = (1-\phi)\rho_s + (1-S)\phi\rho_w + S\phi\rho_h$$

The S-wave velocity of hydrates-bearing sediments is related to the P-wave velocity for clastic sediments (Lee et al. 1996) as

$$V_S = V_P[\alpha(1-\phi) + \beta\phi S + \gamma\phi(1-S)] \quad (2b)$$

where $\alpha = V_s/V_p|_{matrix}$, $\beta = V_s/V_p|_{hydrate}$ and $\gamma = V_s/V_p|_{fluid}$

Variations of V_P, V_S and the Poisson ratio (P) with gas-hydrates saturation are shown in Fig. 2.

Seismic velocity of gas saturated sediments

Gas-hydrates can trap free-gas underneath and the presence of even a small quantity of gas below the BSR reduces the V_P considerably. This makes an appreciable effect on AVA from the BSR. The V_P and V_S for partially gas-saturated hemipelagic sediments can be calculated as (Hegerud et al. 1999)

$$V_P = \sqrt{(K_{sat} + 4/3G_{sat})/\rho_b} \quad \text{and } V_S = \sqrt{G_{sat}/\rho_b} \quad (3)$$

where K_{sat} and G_{sat} are bulk and shear modulus of the sediment saturated with pore fluid of bulk modulus K_f, written as (Gassmann 1951)

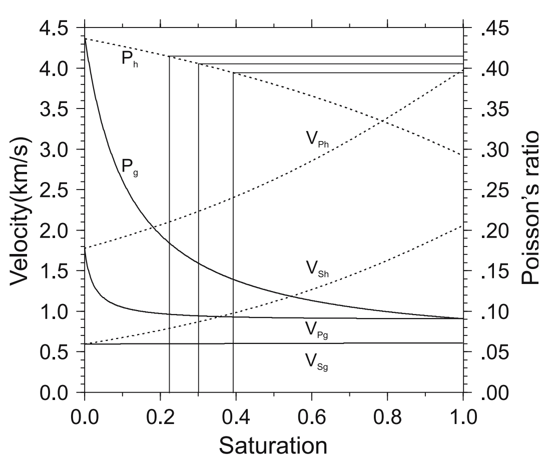

Fig. 2 Variation of P-wave (V_P) and S-wave (V_S) seismic velocities and Poisson's ratio (P) with gas-hydrates (dotted lines) and gas (solid lines) saturation respectively. Subscripts h and g stand for hydrates and gas bearing sediments. Here, we have used $W = 1.82$, obtained by comparing Eq. 2a for 0% hydrates and Eq. 3 for 0% free-gas and $n = 1$. Values of other parameters used for theoretical computation are shown in Table 1

$$K_{sat} = K\left[\frac{\phi K_{dry} - (1+\phi)K_f K_{dry}/K + K_f}{(1-\phi)K_f + \phi K - K_f K_{dry}/K}\right] \quad (4)$$

$$G_{sat} = G_{dry}$$

where K_{dry} and G_{dry} are the bulk modulus and shear modulus of the rock frame with porosity ϕ, and critical porosity ϕ_c respectively, given by the modified lower bound of Hashin-Shtrikman (Dvorkin and Nur 1996) as

$$K_{dry} = \left[\frac{\phi/\phi_c}{K_{hm}+\frac{4}{3}G_{hm}} + \frac{1-\phi/\phi_c}{K+\frac{4}{3}G_{hm}}\right]^{-1} - \frac{4}{3}G_{hm} \quad \text{for } \phi < \phi_c$$

$$= \left[\frac{(1-\phi)}{(1-\phi_c)}\left[\frac{1}{[K_{hm}+\frac{4}{3}G_{hm}]}\right] + \frac{(\phi-\phi_c)}{(1-\phi_c)}\left[\frac{1}{\frac{4}{3}G_{hm}}\right]\right]^{-1} - \frac{4}{3}G_{hm} \quad \text{for } \phi > \phi_c$$

$$G_{dry} = \left[\frac{\phi/\phi_c}{G_{hm}+Z} + \frac{1-\phi/\phi_c}{G+Z}\right]^{-1} - Z \quad \text{for } \phi < \phi_c$$

$$= \left[\frac{(1-\phi)}{(1-\phi_c)}\left[\frac{1}{G_{hm}+Z}\right] + \frac{(\phi-\phi_c)}{(1-\phi_c)Z}\right]^{-1} - Z \quad \text{for } \phi > \phi_c$$

where $Z = \frac{G_{hm}}{6}\left[\frac{9K_{hm}+8G_{hm}}{K_{hm}+2G_{hm}}\right]$, $K_{hm} = [m^2(1-\phi_c{}^2)G^2P/18\pi^2(1-v)^2]^{1/3}$ and

$$G_{hm} = \left[\frac{(5-4v)}{5(2-v)}\right]\left[\frac{3m^2(1-\phi_c^2)G^2P}{2\pi^2(1-v)^2}\right]^{1/3}$$

$P = (\rho_b - \rho_w)gD$ is effective pressure, where g is the acceleration due to gravity and D is the depth.

$v = 0.5(K - 2/3G)/(K + 1/2G)$ is the Poisson's ration of solid phase.

For a matrix consisting of different minerals, the effective elastic constants of solid phase are calculated using Hill's (1952) average formula as

$$K = (1/2)\left[\sum_{i=1}^{L} f_i K_i + \left(\sum_{i=1}^{L} f_i/K_i\right)^{-1}\right] \text{and}$$

$$G = (1/2)\left[\sum_{i=1}^{L} f_i G_i + \left(\sum_{i=1}^{L} f_i/G_i\right)^{-1}\right] \quad (5)$$

where L is the number of mineral constituents and f_i is the volumetric fraction of the ith constituent having bulk modulus K_i and shear modulus G_i in the solid phase. The solid phase density (ρ) and bulk density (ρ_b) are computed as

$$\rho = \sum f_i\rho_i \quad \text{and } \rho_b = (1-\phi)\rho + \phi\rho_w \quad (6)$$

where ρ_i is the density of ith constituent.

Variations of V_P,V_S and the Poisson ratio (P) with free-gas saturation are shown in Fig. 2. Because the sediments in the study area are clay rich (personal communication,

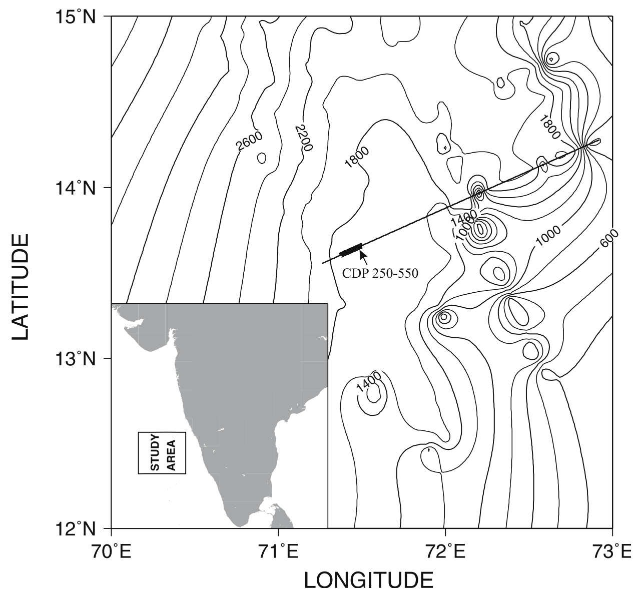

Fig. 3 Location of the study area; western offshore of India. Profile containing CDPs 250–550 are shown by thick solid line. Bathymetry is contoured at every 200 m

ONGCL Personnel), we assume 80% clay and 20% quartz for the mineral constituents in solid phase.

Data

We apply the AVA modeling to a field data set in the Kerala-Konkan Basin (Fig. 3) where the presence of a BSR has already been established (Reddi et al. 2001; Rao et al. 2001; Satyavani et al. 2002; Shankar et al. 2004). The details of data acquisition and processing are available in these references. Figure 4 shows a seismic section along the line between CDPs (common depth points) 250–550, which shows a clear BSR at about 2.9–2.95 s TWT (two way time). The water depth is ~2.0 km, whereas the maximum offset of the data is limited to 2.6 km. For AVA modeling, we select three interfaces, such as the seafloor, BSR and a reflector between the seafloor and the BSR. We use CDPs 350–400 where the BSR shows quite strong reflection. Depths to various reflectors are obtained from the conversion of RMS (root mean square) velocity versus TWT function into interval velocity-depth function using the well-known Dix's formula (Dix 1955). Fig. 5 displays one representative gather at CDP 371 that shows the reflections from three horizons and the first multiple of seafloor reflection as a function of offsets. The spiking deconvolution, spherical divergence correction, bandpass filtering and detailed velocity analysis have been carried out before picking amplitudes from NMO (normal move out) corrected CDP gathers in which the reflector gets horizontally aligned. The amplitudes of the seafloor reflection are converted into reflection coefficients (R_s) using Warner's (1990) approach as

$$R_s = A_m/A_p \tag{7}$$

where A_m = the amplitude of the first multiple of the seafloor reflection.

A_p = the amplitude of the seafloor reflection.

The BSR reflection coefficient is calculated as

$$R_{bsr} = \frac{A_{bsr}}{A_p} R_s$$

where A_{bsr} = the amplitude of the BSR.

In a similar way, reflection coefficients of the reflector above the BSR are calculated. To correct the transmission losses at the seafloor, reflection coefficients of reflectors below the seafloor are multiplied by the factor$1/(1–R_s^2)$ (Fink and Spence 1999). The reflection coefficients associated with the three reflectors are shown in Fig. 6.

Fig. 4 Seismic section between CDPs 250–550 in the study region. Various reflectors are marked in the section

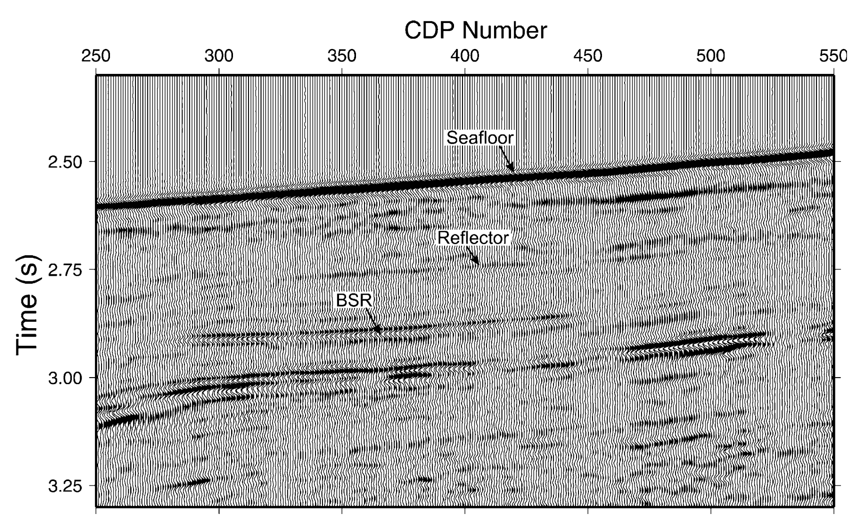

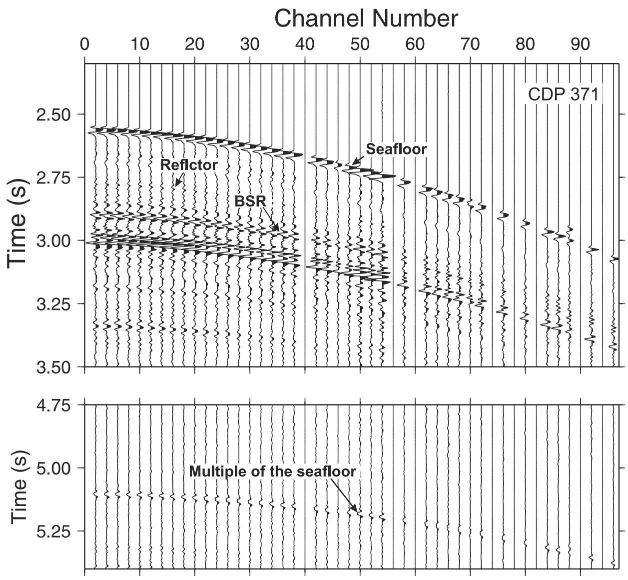

Fig. 5 A representative CDP gather (without NMO correction), which shows variation of amplitudes with offsets for three reflectors. Lower portion shows the amplitude variation of first multiple of the seafloor reflection with offsets

AVA Modeling

To avoid field errors caused by several factors, we average out the reflection coefficients for each reflector (shown by asterisks in Fig. 6) for AVA modeling. Since densities are in ratio in Eq. 1 and the seismic data (originally recorded for conventional hydrocarbon prospecting) have limited offset, it is difficult to determine all six elastic parameters across an interface simultaneously. We perform constrained AVA modeling by minimizing the RMS residual between the observed and the calculated reflection coefficients, computed using Eq. 1. We fix V_P, V_S and ρ as 1.5 km/s, 0.001 km/s and 1.0 g/cc respectively for the seawater and determine three elastic parameters of the sediments at the seafloor (Table 2) corresponding to an RMS residual of 0.0041. By holding fixed the above three derived parameters as top parameters, we determine the bottom three parameters associated with the reflector above the BSR. The RMS residual and the estimated parameters are shown in Table 2. Since the BSR is a physical property interface, not a lithological boundary, the layer stripping approach is modified slightly while modeling the seismic reflection data from the BSR. The top of the gas-hydrates saturated layer is gradational in nature and hard to identify on seismic data. In addition, concentrations of gas-hydrates increase with depth. This, in turn, increases both the V_P and V_S with depths, which reach a maximum at the BSR. Presence of free-gas below the BSR decreases the V_P considerably but does not affect the V_S. So the V_S below the BSR can be considered as that derived for the bottom layer

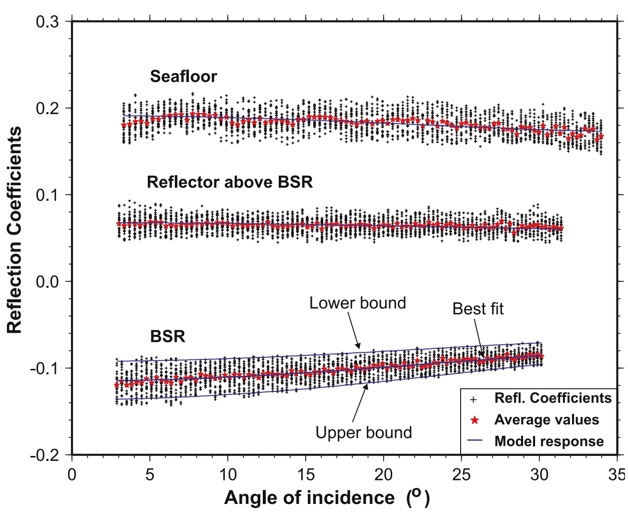

Fig. 6 Reflections coefficients (plus symbols) for seafloor, a reflector above the BSR and BSR respectively between CDPs 350–400. Average reflection coefficients (asterisks), used for modeling. The theoretical responses (solid lines), computed using the Zoeppritz equation, are superimposed on the observed data to demonstrate the fit between them. Lower and upper bounds (shown by arrows) reflection coefficients are modeled to estimate the lower- and upper-bound errors of gas-hydrates saturation

Table 1 Quantities used to compute seismic velocities in partially gas-saturated sediments (Lee and Collett 2001)

Parameters	Values and units
Bulk modulus of quartz	36 GPa
Shear modulus of quartz	45 GPa
Bulk modulus of clay	20.9 GPa
Shear modulus of clay	6.85 GPa
Bulk modulus of pure gas-hydrate	7.9 GPa[a]
Shear modulus of pure gas-hydrate	2.25 GPa[a]
Bulk modulus of methane	0.33 GPa[b]
Bulk modulus of water	2.25 GPa
Density of quartz	2.65×10^3kg/m^3
Density of clay	2.58×10^3kg/m^3
Density of pure gas-hydrate	0.92×10^3kg/m^3
Density of methane	0.112×10^3kg/m^3 [b]
Density of seawater	1.0×10^3kg/m^3
Acceleration due to gravity	9.81 m/s^2
Depth to the BSR below seabed	450.00 m
Sediment porosity	0.4
Critical porosity of sediment	0.38
A constant simulating the lithification rate with hydrates concentration	1
P-wave velocity of the water	1.5 km/s
No of grain/contact	9

[a] Helgerud et al. (1999)

[b] Dvorkin and Nur (1996)

Table 2 Model parameters estimated by AVA modeling

Reflectors	V_{P1}/V_{P2}	V_{S1}/V_{S2}	ρ_1/ρ_2	RMS error
Seafloor	1500/1696	0.001/491	1030/1342	0.0041
Reflector above the BSR	1696/1770	491/545	1342/1472	0.0022
BSR	2245/1780	895/545	1472/1472	0.0026

of the reflector above the BSR. The density of gas-hydrates-bearing sediments and free-gas saturated sediments across the BSR remains almost the same as that of the background density. The density derived for the bottom layer of the reflector above the BSR can be assumed to be the background density.

The Zoeppritz equation has two parts: (i) the zero angle reflection coefficient $((V_{P2}/V_{P1} - 1)/(V_{P2}/V_{P1} + 1))$, which is governed by the P-wave velocity ratio at zero density contrast across the BSR, and (ii) the angle dependent reflection coefficient, which is governed by the Poisson's ratio. The zero angle response will be the same as long as the ratio of V_{P2} and V_{P1} remains the same. However in each case, the V_S and hence the Poisson ratio of gas-hydrates-bearing sediments will be different. Models with different values of V_{P1},V_{P2} and V_{S1} will produce the same AVA responses from the BSR. But, there will be only one solution if we constrain the V_S with V_P through Eq. 2b for the gas-hydrates-bearing sediments. Thus the AVA modeling of BSR, in which V_P and V_S (related by Eq. 2b) of the gas-hydrates laden sediments and V_P of the underlying sediments are determined, does not have any ambiguity. The P-wave velocity of gas-hydrates and free-gas saturated sediments across the BSR are estimated as 2.245 and 1.78 km/s respectively. The S-wave velocity above the BSR is calculated as 0.895 km/s. This corresponds to a Poisson ratio of 0.406 and gas-hydrates saturation of ~30% (Fig. 2). The P-wave velocity (1.77 km/s) of the bottom layer of the reflector above the BSR can be considered as the background velocity of the sediments. Because the P-wave velocity (1.77 km/s) of the background sediment and the P-wave velocity (1.78 km/s) below the BSR are almost equal, we can infer that the origin of BSR is mainly due to the presence of gas-hydrates. The absence of free-gas below the BSR is also qualitatively understood from the decreasing nature of absolute value of negative reflection coefficients with angles (Carcione and Tinivella 2000) for the BSR (Fig. 6).

As the field data in Fig. 6 are scattered, the AVA modeling is not complete unless we provide an error-estimate of gas-hydrates saturation. For this purpose, we perform the AVA modeling through the lower-bound and upper-bound reflection coefficients (Fig. 6), which show the lower-limit of 22% and upper-limit of 38% for gas-hydrates saturation respectively.

Conclusions

Because the seismic data, available for this study is of limited offset, we can not derive all six elastic parameters associated with a reflector simultaneously. To estimate elastic parameters from such a data set, we use an approach of constrained AVA modeling. The approach is applied to a seismic data set in the Kerala-Konkan Basin located on the western continental margin of India where the presence of BSR has already been established. The best fit modeling through the averaged reflection coefficients shows P- and S-wave seismic velocities of 2.245 and 0.895 km/s respectively, and the Poisson's ratio of 0.406 for the gas-hydrate-bearing sediment. This corresponds to the gas-hydrate saturation of 30 ± 8%. By comparing the P-wave velocity of 1.78 km/s for the sediment below the BSR to that (1.77 km/s) above the gas-hydrates-bearing sediment, we conclude that the BSR in the Kerala-Konkan region is mainly caused by the presence of gas-hydrates, because presence of free-gas would have resulted in lower P-wave velocity than that seen as the background velocity and an increase in absolute value of negative reflection coefficients with angles.

Acknowledgements We thank the Director, NGRI for his kind permission and Dr. N.K. Thakur for discussion. We also thank the Department of Science & Technology, New Delhi, India for financial support through an award of Swarnajayanti Project to KS. We are grateful to editor in Chief Peter Clift, editor Dr. John Chen, and an anonymous reviewer for their comments and suggestions to improve the quality of the paper.

References

Carcione JM, Tinivella U (2000) Bottom-simulating reflectors: seismic velocities and AVO effects. Geophysics 65:54–67

Castagna JP, Batzle ML, Kan TK (1993) Rock physics: the link between rock properties and AVO response. In: Castagna JP, Backus MM (eds) Offset-dependent reflectivity-theory and practice of AVO analysis. Soc Expl Geophys, pp 135–171

Dix CH (1955) Seismic velocities from surface measurements. Geophysics 20:68–86

Dvorkin J, Nur A (1996) Elasticity of high-porosity sandstones: theory for two north sea datasets. Geophysics 61:1363–1370

Fink CR, Spence GD (1999) Hydrate distribution off Vancouver Island from multifrequaency single-channel seismic reflection data. J Geophys Res 04:2909–2922

Helgerud MB, Dvorkin J, Nur A, Sakai A, Collett T (1999) Elastic-wave velocity in marine sediments with gas hydrates: effective medium modeling. Geophys Res Lett 26:2021–2024

Hill R (1952) The elastic behavior of crystalline aggregate. Proc Phys Soc London A65:349–354

Henriet JP, Mienert J (eds) (1998) Gas hydrates: relevance to the world margin stability and climate change. Geological Society London, Special Publications

Lee MW, Collett TS (2001) Elastic properties of gas hydrate-bearing sediments. Geophysics 66:763–771

Lee MW, Hutchinson DR, Collett TS, Dillon WP (1996) Seismic velocities for hydrate-bearing sediments using weighted equation. J Geophys Res 101:20347–20358

Max MD (2003) Natural gas hydrate in oceanic and permafrost environments. Kluwer Academic Publisher, Dordrecht, The Netherlands

Paul CK, Dillon WP (2001) Natural gas hydrates: occurrence, distribution and detection geophysical monograph. AGU, Washington

Ostrander WJ (1984) Plane-wave reflection coefficients for gas sands at non-normal angles of incidence. Geophysics 49:1637–1649

Rao YH, Subrahmanium C, Rastogi A, Deka B (2001) Anamalous features related to gas/gas hydrate occurrences along the western continental margins of India. Geo Mar Lett 21:1–8

Reddi S, Thakur NK, Ashalatha B, Sain K (2001) Reprocessing of multichannel seismic data of ONGCL for gas-hydrate investigation in offshore Goa, (Part-II: Special Processing) NGRI Tech. Rep. No. NGRI-2001-EXP-307 (Unpublished)

Satyavani N, Shankar U, Thakur NK, Reddi SI (2002) Probable gas hydrate/free gas model over the western continental margin of India. Mar Geophys Res 23:423– 430

Shankar U, Satyavani N, Sinha B, Thakur NK (2004) Seismic reflection data: their utility in estimation of gas hydrates in deep marine sediments. Curr Sci 87:515–520

Sloan ED (1998) Clathrate hydrate of natural gases. Marcel Dekker Inc, New York

Warner M (1990) Absolute reflections from deep seismic reflections. Tectonophysics 173:15–23

Waters KH (1997) Reflection Seismology, 1st edn. A Wiley Interscience Publication, California, pp 6–42

Wood AB (1941) A textbook of sound. Macmillan, New York, pp 578

Wyllie MRJ, Gregory AR, Gardner GHF (1958) An experimental investigation of factors affecting elastic wave velocities in porous media. Geophysics 23:459–493

Zoeppritz K (1919) On the reflection and penetration of seismic waves through unstable layers. In: Goettinger Nachr (ed) Erdbebenwellen VIII B, pp 66–84